Anal. Chem. **1999,** *71,* 3918−3927

Articles

Gas-Phase Separations of Electrosprayed Peptide Libraries

Catherine A. Srebalus,[†] Jianwei Li,[†] William S. Marshall,[‡] and David E. Clemmer*,[†]

Department of Chemistry, Indiana University, Bloomington Indiana 47405, and Amgen Inc., 3200 Walnut Street, Boulder, Colorado 80301

High-resolution ion mobility spectrometry has been combined with time-of-flight mass spectrometry for analysis of a combinatorial peptide library that is expected to contain 676 components. In this approach, the components of a mixture of three residue peptides, having the general form (D)Phe-Xxx-Xxx-$CONH_2$ (where Xxx is randomized over 26 residues including 10 naturally occurring amino acids and 16 synthetic forms) were ionized by electrospray ionization. Ion mobility/time-of-flight distributions have been recorded for all ions using a nested drift(flight) time technique. The improvement in resolving power [$(t/\Delta t) = 100-150$ for singly charged ions] was illustrated by analysis of a mixture of tryptic digest peptides using high- and low-resolution instruments. The approach allows many components of the library (e.g., structural, sequence, and stereo isomers) that cannot be distinguished by mass spectrometry alone to be resolved. Impurities due to side reactions appear to be minimal, comprising <10% of the total ion signal. Direct evidence for ~60−70% of the expected peptides is found. Variation in ion abundance for different components indicates that there are differences in solution concentrations or ionization efficiencies for the components.

Mix and split strategies for synthesis of diverse mixtures[1] are currently used in many combinatorial approaches for identifying molecules with potential pharmacological importance.[2] Few analytical methods are capable of analyzing large libraries of related molecules (especially isomers) on reasonable time scales; for this reason, the identities and quantities of individual components in mixtures containing more than a few dozen components are usually unknown. A concern that arises during library synthesis is that if synthetic steps fail, screening strategies could produce false-negative results; entire families of potentially important molecules could be missed. Additionally, unexpected side reactions may lead to positive results that are difficult to identify on the basis of the expected composition of the mixture.

Mass spectrometry (MS)-based methods can be used to rapidly assess abundance information for ions with different m/z ratios that are present in mixtures, including combinatorial libraries.[3,4] However, information about species with identical m/z ratios (isomer abundance) is inferred by comparing peak heights for different m/z ions;[5,6] this assumes that each component in the mixture is present in equal abundance and has the same ionization efficiency. Most components generated by mix and split syntheses will coexist with other sequence, structural, or stereo isomer forms. For example, a peptide scaffold, such as Ala-Xxx-Lys-Xxx-Leu-Xxx-Xxx-Ala, with four variable sites, randomized over five possible residues, will lead to a library of 4^5 or 1024 different components; only $(5+4-1)!/4!(5-1)!$ or 70 different m/z ratios are possible.[7] Usually, fewer peaks are discernible because of limitations in experimental resolving power and the fact that many synthetic residues (or combinations of residues) have identical (or indistinguishable) molecular weights [i.e., combinations of residues [e.g., Ala-Val (mol wt 170.2121) ≈ Gly-Ile (mol wt 170.2120)]; isomeric residues [e.g., Ile and Leu]; and D- and L-stereoisomers]. Complications associated with ionization, such as the multiple charging phenomenon that arises during electrospray ionization[8] (ESI) for some peptides, or the generation of matrix ions during matrix-assisted laser desorption/ionization

[†] Indiana University.

[‡] Amgen Inc.

(1) Lebl, M.; Krchnak, V. *Methods Enzymol.* **1997**, *289*, 336.

(2) Gallop, M. A.; Barrett, R. W.; Dower, W. J.; Fodor, S. P. A.; Gordon, E. M. *J. Med. Chem.* **1994**, *37*, 1233. Gordon, E. M.; Barrett, R. W.; Dower, W. J.; Fodor, S. P. A.; Gallop, M. A. *J. Med. Chem.* **1994**, *37*, 1385. Pavia, M. R.; Sawyer, T. K.; Moos, W. H. *Bioorg. Med. Chem. Lett.* **1993,** *3*, 387. Houghten, R. A. *Trends Genet.* **1993**, *9*, 235. Scott, J. K. *Trends Biol. Sci.* **1992**, *17*, 241. Moos, W. H.; Green, G. D.; Pavia, M. R. In *Annual Reports in Medicinal Chemistry*; Bristol, J. A., Ed.; Academic Press: San Diego, CA, 1993.

(3) Chu, Y.-H.; Dunayevskiy, Y. M.; Kirby, D. P.; Vouros, P.; Karger, B. L. *J. Am. Chem. Soc.* **1996**, *118*, 7827. Loo, J. A. *Eur. Mass Spectrom.* **1997**, *3*, 93. Dunayevskiy, Y. M.; Lai, J.-J.; Quinn, C.; Talley, F.; Vouros, P. *Rapid Commun. Mass Spectrom.* **1997**, *11*, 1178. Wigger, M.; Nawrocki, J. P.; Watson, C. H.; Eyler, J. R.; Benner, S. A. *Rapid Commun. Mass Spectrom.* **1997**, *11*, 1749. Wieboldt, R.; Zweigenbaum, J.; Henion, J. *Anal. Chem.* **1997**, *69*, 1683.

(4) Nawrocki, J. P.; Wigger, M.; Watson, C. H.; Hays, T. W.; Senko, M. W.; Benner, S. A.; Eyler, J. R. *Rapid Commun. Mass Spectrom* **1996**, *10*, 1860.

(5) Metzger, J. W.; Kempter, C.; Wiesmuller, K. H.; Jung, G. *Anal. Biochem.* **1994**, *219*, 261.

(6) Andrews, P. C.; Boyd, J.; Ogorzalek Loo, R.; Zhao, R.; Zhu, C. Q.; Grant, K.; Williams, S. In *Techniques in Protein Chemistry V*; Crabb, J. W., Ed.; Academic Press: San Diego, 1994; p 485.

(7) Constantine, G. *Combinatorial Theory and Statistical Design*; John Wiley & Sons: New York, 1987. Demirev, P. A.; Zubarev, R. A. *Anal. Chem.* **1997**, *69*, 2893.

(8) Fenn, J. B.; Mann, M.; Meng, C. K.; Wong, S. F.; Whitehouse, C. M. *Science* **1989**, *246*, 64.

10.1021/ac9903757 CCC: $18.00
Published on Web 08/18/1999

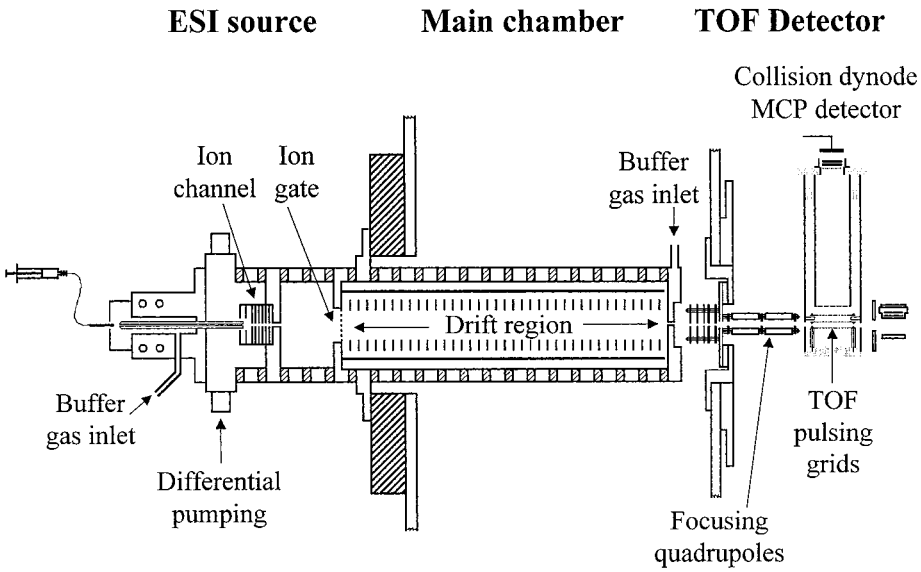

Figure 1. Schematic diagram of the high-resolution ion mobility time-of flight mass spectrometer.

(MALDI),[9] can further obscure information about library composition.

In this paper, we have combined a high-resolution drift tube with time-of-flight mass spectrometry to analyze a tripeptide library having the general form (D)Phe-Xxx-Xxx-$CONH_2$, where Xxx is randomized over 26 different amino acids (10 naturally occurring residues and 16 synthetic forms); thus, 676 (26^2) different peptides are expected to be present in the mixture. All components of the mixture are electrosprayed into a high-pressure buffer gas. The ions are subjected to a weak electric field and separated on the basis of differences in their mobilities through the buffer gas prior to entering a time-of-flight mass spectrometer for m/z analysis. Recently we have shown that mixtures of peptides from tryptic digestion of proteins can be rapidly analyzed with an analogous approach that utilizes a low-resolution drift tube.[10,11] The mobility separation significantly reduces spectral congestion and peaks often fall into families determined by the ion charge state.[10] Below, we present the first high-resolution spectrum for a tryptic digestion of sheep albumin (a 66 kDa protein). In addition to charge-state separation, it is possible to disperse components having similar molecular weights within a single charge-state family. Charge-state families are also observed in the peptide library data. The gas-phase mobility separation[12,13] allows differentiation of many structural, sequence, and stereo isomers that could not be resolved by MS alone.

EXPERIMENTAL METHODS

General Information. Detailed discussions of ion mobility-MS methods[12] and their applications to biomolecules have been given previously.[13–16] Only a brief description is given here. Figure 1 shows a schematic diagram of the experimental apparatus. A mixture of peptides is electrosprayed at atmospheric pressure and introduced into the instrument through a differentially pumped capillary inlet system.[17] Ion mobility distributions are recorded by measuring the time required for a pulse of ions to travel across a well-defined drift region under the influence of a uniform electric field. Ions that exit the drift tube are focused into a time-of-flight (TOF) mass spectrometer and detected. Because drift times for ions through the buffer gas are significantly longer (milliseconds) than flight times in the time-of-flight region of the instrument (microseconds), multiple TOF mass spectra can be acquired for a single pulse of ions into the drift tube.[18] Simultaneous acquisition of mobility and m/z data allows rapid separation and mass identification of mixture components.

Preparation of Tryptic Digest Mixture. A peptide mixture from a tryptic digest of sheep albumin (Sigma) was generated by addition of 150 μL of a 0.2 mg mL^{-1} trypsin (Sigma, sequencing grade) solution in 0.2 M ammonium bicarbonate (EM Science) to 0.5 mL of a 20.0 mg mL^{-1} solution of sheep albumin. After incubation for 20 h at 37 °C, the trypsin was filtered from the digest using a microconcentrator (Microcon 10, Amicon, Inc.) and

(9) Karas, M.; Hillenkamp, F. *Anal. Chem.* **1988**, *60*, 2299.
(10) Valentine, S. J.; Counterman, A. E.; Hoaglund, C. S.; Reilly, J. P.; Clemmer, D. E. *J. Am. Soc. Mass Spectrom.* **1998**, *9*, 1213.
(11) Henderson, S. C.; Valentine, S. J.; Counterman, A. E.; Clemmer, D. E. *Anal. Chem.* **1999**, *71*, 291.
(12) Ion mobility spectrometry methods are discussed in the following references: Hagen, D. F. *Anal. Chem.* **1979**, *51*, 870. Tou, J. C.; Boggs, G. U. *Anal. Chem.* **1976**, *48*, 1351. Karpas, Z.; Cohen, M. J.; Stimac, R. M.; Wernlund, R. F. *Int. J. Mass Spectrom. Ion Processes* **1986**, *74*, 153. St. Louis, R. H.; Hill, H. H. *Crit. Rev. Anal. Chem.* **1990**, *21*, 321. von Helden, G.; Hsu, M. T.; Kemper, P. R.; Bowers, M. T. *J. Chem. Phys.* **1991**, *95*, 3835. Jarrold, M. F. *J. Phys. Chem.* **1995**, *99*, 11.
(13) For recent reviews of ion mobility studies of biomolecules, see: Clemmer, D. E.; Jarrold, M. F. *J. Mass Spectrom.* **1997**, *32*, 577. Liu, Y.; Valentine, S. J.; Counterman, A. E.; Hoaglund, C. S.; Clemmer, D. E. *Anal. Chem.* **1997**, *69*, 728A.
(14) Clemmer, D. E.; Hudgins, R. R.; Jarrold, M. F. *J. Am. Chem.* Soc. **1995**, *117*, 10141. Shelimov, K. B.; Clemmer, D. E.; Hudgins, R. R.; Jarrold, M. F. *J. Am. Chem. Soc.* **1997**, *119*, 2240. Shelimov, K. B.; Jarrold, M. F. *J. Am. Chem. Soc.* **1997**, *119*, 9586.
(15) Valentine, S. J.; Clemmer, D. E. *J. Am. Chem. Soc.* **1997**, *119*, 3558. Valentine, S. J.; Anderson, J.; Ellington, A. E.; Clemmer, D. E. *J. Phys. Chem. B* **1997**, *101*, 3891. Valentine, S. J.; Counterman, A. E.; Clemmer, D. E. *J. Am. Soc. Mass Spectrom.* **1997**, *8*, 954.
(16) von Helden, G.; Wyttenbach, T.; Bowers, M. T. *Science* **1995**, *267*, 1483. Lee, S.; Wyttenbach, T.; von Helden, G.; Bowers, M. T. *J. Am. Chem. Soc.* **1995**, *117*, 10159. Wyttenbach, T.; von Helden, G.; Bowers, M. T. *J. Am. Chem. Soc.* **1996**, *118*, 8355.
(17) Counterman, A. E.; Valentine, S. J.; Srebalus, C. A.; Henderson, S. C.; Hoaglund, C. S.; Clemmer, D. E. *J. Am. Soc. Mass Spectrom.* **1998**, *9*, 743.
(18) Hoaglund, C. S.; Valentine, S. J.; Sporleder, C. R.; Reilly, J. P.; Clemmer, D. E. *Anal. Chem.* **1998**, *70*, 2236.

the peptides that remained were lyophilized.

Synthesis of Peptide Libraries. The (D)Phe-Xxx-Xxx-$CONH_2$ library was synthesized using a mix and split strategy[1] employing a gas (N_2)-agitated manifold system using standard Fmoc chemistry protocols.[19] The following appropriately protected library inputs were used: isoleucine (Ile, mol wt = 113.2), tyrosine (Tyr, 163.2), tryptophan (Trp, 186.2), serine (Ser, 87.1), histidine (His, 137.1), proline (Pro, 97.1), aspartic acid (Asp, 115.1), arginine (Arg, 156.2), lysine (Lys, 128.2), glutamine (Gln, 128.1), D-asparagine [(D)Asn, 114.1], D-glutamic acid [(D)Glu, 129.1], D-alanine [(D)-Ala, 71.1], D-phenylalanine [(D)Phe, 147.2], D-lysine [(D)Lys, 128.2], hydroxyproline (Hyp, 113.1), β-alanine [(β)Ala, 71.1], aspartic(*O*-benzyl) acid [Asp(Obzl), 205.2], glutamic(*O*-benzyl) acid [Glu-(Obzl), 219.3], benzyl histidine [His(Bzl), 227.3], β-(1-naphthyl)-alanine [(*N*)Ala, 197.2], β-(3-pyridyl)alanine [(*3*)Ala, 148.2], *p*-nitrophenylalanine [(*P*)Ala, 192.2], β-cyclohexylalanine (Chex, 153.3), γ-aminobutyric acid [(γ)Abu, 85.1], and tetrahydroisoquinoline-3-carboxylic acid (TIC, 159.2).

The library was synthesized as follows. Equimolar quantities of Knorr-MBHA resin (Colorado Biotechnology Associates, Casper, WY), loaded with each of the 26 residues, were combined to generate 0.3 mmol of total peptide equivalents. The resulting resin was thoroughly mixed by a 2-h agitation in dichloromethane (DCM) followed by dimethylformamide (DMF), washed five times with methanol, vacuum-dried, and evenly distributed into 26 individual reaction vessels for the second coupling. The α-amino Fmoc group of the peptide resin in each vessel was removed using 20% piperidine in DMF prior to the addition of the next amino acid. Subsequent residues were added to the resin in each reaction vessel using a single 3-h coupling of 2 equiv of the hydroxybenzotriazole (HOBt) ester of the appropriate amino acid. Coupling efficiencies were monitored using the ninhydrin test,[20] and additional couplings were performed as necessary. Following the second amino acid coupling, the resins were mixed (as described above) and deprotected, and the final (D)Phe residue was attached in an analogous procedure. The resulting resin mixture was Fmoc deprotected and the tripeptides were cleaved from the resin by suspension in a 5% water, 5% phenol, 5% thioanisole, 5% β-mercaptoethanol, 80% trifluoroacetic acid solution (10 mL) for 3 h. Following peptide cleavage, the resin was washed twice with DCM, the combined filtrates were concentrated by rotoevaporation, and the library peptides were precipitated using ether. The precipitate was dissolved in 50:50 water/acetonitrile, frozen, and lyophilized. The presence of naturally occurring amino acids was verified by amino acid analysis.

Electrospray of Mixtures. Solutions of the tryptic digest and peptide library mixtures were prepared by dissolving ~1 mg of the mixture in 2.0 mL of water. This solution was diluted to a final concentration of 0.25 mg mL^{-1} in 49:49:2 water/acetonitrile/acetic acid solution (by volume) and electrosprayed in positive ion mode using a solution flow rate of 1.7 μL min^{-1}.

Ion Source. Ions are electrosprayed at atmospheric pressures directly into a differentially pumped desolvation region through a 17.8-cm-long, 0.16-cm-diameter capillary tube. Ions are forced through the tube by the pressure gradient across the capillary. This basic design is similar to one described by Guevremont and co-workers.[21] The capillary extends into the center of a series of 10 BeCu lenses separated by 0.10-in.-thick Teflon spacers. The lenses and spacers create a 0.2-cm-diameter channel that is ~2.5 cm long; most of the He buffer gas is pumped away through this region via the differentially pumped ion source. We estimate that the pressure in the differential pumping region is ~200−250 Torr. The lenses are connected by a series of resistors in order to create a uniform electric field, and the voltage drop across these lenses is ~1000−2000 V. This field guides the ions from the source into the body of the drift tube against the counterflow of He buffer gas, while preventing neutrals from entering the drift region.[22] Once inside the body of the drift tube, the ions drift through the buffer gas under the influence of a field provided by the copper ring electrodes. Pulses of ions for mobility experiments are introduced using a method that is similar to that discussed previously by Hill and co-workers.[12d] Typical experimental repetition rates are 20 Hz, such that experimental duty cycles range from 0.04 to 0.1%.

High-Resolution Drift Tube. Recently, the resolving powers of ion mobility instruments have been improved substantially; values of $t_D/\Delta t > 170$ (where t_D is the drift time of the ion through the instrument and Δt is the full width at half-maximum of the peak) for singly charged ions have been reported.[22,23] The drift field is created by voltages that are applied to a series of 0.010-in.-thick BeCu rings that are connected in series by 5.00 MΩ high-vacuum resistors (KDI Electronics, 1%). The pressure of the He buffer gas is typically 150.0−300.0 Torr and can be regulated to within ±0.05 Torr during experiments.

Mass Spectrometer. When ions exit the drift tube they enter an einzel/dc-quadrupole lens system that is designed to focus the ion beam into the shape of a ribbon. Ions travel ~25 cm across this focusing region and exit through a slit (0.16 × 1.27 cm) into the extraction region of the TOFMS instrument. Pressures in this region are $<10^{-6}$ Torr. Voltages associated with the TOF source extraction grids and the 17.5-cm-long field-free flight tube were established by an algorithm that has been described previously.[24] Ions are detected by a pair of microchannel plates mounted directly to the back of the flight tube.

Ion Mobility and TOF Considerations. We refer to the term *drift time* as the time required for ions to travel through the high-pressure drift tube as given by[25]

$$t_D = L/E_D K \qquad (1)$$

where K is the mobility of the ions, L is the length of the drift tube, and E_D is the applied drift field. The term *flight time* refers to the time required for ions that have been accelerated to a desired kinetic energy in a vacuum to travel through the field-free region of the mass spectrometer. The flight time is

(19) Wellings, D. A.; Atherton, E. *Methods Enzymol.* **1997**, *289*, 44.
(20) Kaiser, E.; Colescott, R. L.; Bossinger, C. D.; Cook, P. I. *Anal. Biochem.* **1970**, *34*, 595.
(21) Guevremont, R.; Siu, K. W. M.; Wang, J.; Ding, L. *Anal. Chem.* **1997**, *69*, 3959.
(22) Dugourd, P.; Hudgins, R. R.; Clemmer, D. E.; Jarrold, M. F. *Rev. Sci. Instrum.* **1997**, *119*, 2240.
(23) Hill and co-workers have reported that the resolving power for peaks associated with highly charged protein ions can exceed 200. See: Wu, C.; Siems, W. F.; Asbury, G. R.; Hill, H. H. *Anal. Chem.* **1998**, *70*, 4929.

$$t_F = l(m/2zeE_{TOF})^{1/2} \quad (2)$$

where l is the length of the field-free region, m is the ion mass, ze is the ion's charge, and E_{TOF} is the kinetic energy of the ions.

Simultaneous measurements of mobilities and m/z ratios are feasible because flight times are much shorter than drift times. This allows flight times of the different m/z ions to be measured within individual time windows of the ion mobility spectrum in a synchronous fashion as described in detail previously.[18] This is referred to as a nested measurement. We usually denote drift and flight times as $t_D(t_F)$ (in units of ms and μs, respectively); in this paper, the time-of-flight axis has been converted to an m/z scale using the relation in eq 2. Contour plots of the data were created using the MATLAB software.[26]

Experimental and Theoretical Ion Mobility Resolving Power. The ability to resolve two ions having different collision cross sections can be expressed as[27]

$$t_D/\Delta t \approx [LEze/(16k_bT \ln 2)]^{1/2} \quad (3)$$

where Δt is the width of the drift time peak at half-maximum; L and T correspond to the measured drift tube length and buffer gas temperature, respectively; and k_b is Boltzmann's constant. We typically use drift fields ranging from ~150 to 280 V cm^{-1}. The drift field is ultimately limited by the discharge potential of the buffer gas at a given operating pressure and temperature.

Figure 2 shows an example high-resolution ion mobility distribution that was obtained by negative ion electrospray of a small organic hexamer, $CH_3(SO_2NHSO_2(CH_2)_6)_5SO_2NHSO_2CH_3$ (gift from B. Burlingham, and T. Widlanski, Indiana University), from a 10^{-5} M 49:49:2 water/acetonitrile/ammonium hydroxide solution. These data were recorded using a high-resolution drift tube/quadrupole mass analyzer configuration detailed elsewhere.[17] From several studies where specific m/z ratios were selected using the quadrupole, we determined that the prominent peaks at 9.0, 10.6, 13.0, and 15.5 ms correspond to $[M - 6H]^{6-}$ $[M - 5H]^{5-}$ $[M - 4H]^{4-}$, and $[M - 3H]^{3-}$ ions, respectively. Analysis of several of the very sharp peaks yields resolving powers ranging from $t/\Delta t$ = 130 to 260, as indicated. To our knowledge, $t/\Delta t = 260$ is the highest resolving power that has been obtained in ion mobility experiments.

A measure of our ability to achieve the theoretical resolving power can be obtained from comparing experimental peaks to peak shapes that are calculated for the transport of a single geometric structure through the drift tube. This is given by[25]

$$\Phi(t) = \int \frac{C}{(Dt)^{1/2}}(v_D + L/t)\left[1 - \exp\left(\frac{-r_o^2}{4Dt}\right)\right] \times \exp\left(\frac{-(L - v_D t)^2}{4Dt}\right) P(t_p)\, dt_p \quad (4)$$

where $\Phi(t)$ is the intensity of ions passing through the exit aperture as a function of time, r_o is the entrance aperture radius, v_D is the measured drift velocity, C is a constant, $P(t_p)\, dt_p$ is the distribution function for the pulse of ions entering the drift tube, and D is the diffusion constant.[28] Experimental peaks that are significantly broader than the calculated distribution indicate that multiple conformations exist, that conformers interconvert as they travel through the buffer gas, or that the experimental parameters are unstable over the time scale of the measurement. Close agreement between the calculated and experimental peaks suggests that only a single conformation is present; however, we cannot rule out the possibility that multiple conformations with identical mobilities are present. The inset in Figure 2 shows a comparison of the theoretical and experimental peak shapes for the $[CH_3(SO_2NHSO_2(CH_2)_6)_5SO_2NHSO_2CH_3 - 4H]^{4-}$ ion. The high experimental resolving power ($t/\Delta t = 240$) that is observed is near the limit imposed by diffusional broadening and the initial ion pulse width. Similar considerations for singly protonated ions give $t/\Delta t \approx 150$, which is often achieved for small peptide ions.

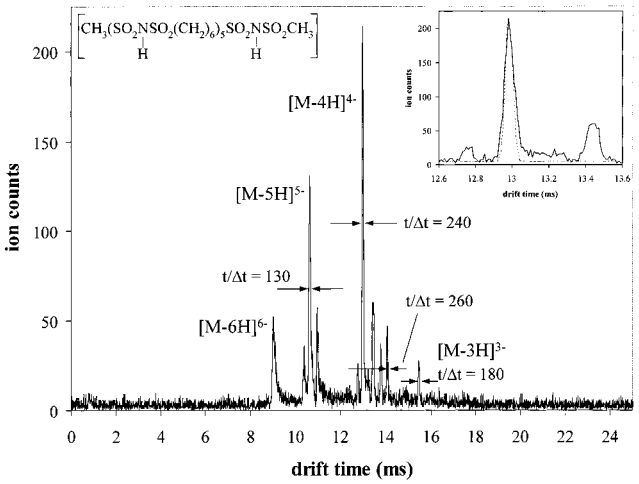

Figure 2. High-resolution ion mobility distribution for all negative ions formed upon electrospraying a 10^{-5} M $CH_3(SO_2NHSO_2(CH_2)_6)_5SO_2NHSO_2CH_3$ in 49:49:2 water/acetonitrile/ammonium hydroxide solution. The major peaks correspond to the $[M - 4H]^{4-}$, $[M - 5H]^{5-}$, and $[M - 6H]^{6-}$ ions, as determined by separate selected-ion experiments. The applied drift field was 200.7 V cm^{-1}, and the He buffer gas pressure was 244.0 ± 0.1 Torr. Experimental resolving powers are indicated for several peaks. The inset shows an expanded view of the $[M - 4H]^{4-}$ peak. The dashed line shows the theoretical peak shape calculated for transport of a single conformation from eq 4, which assumes that peak broadening is due exclusively to diffusion.

Experimental Mobilities. Ion mobility results are often reported in terms of reduced mobilities, as given by[25]

$$K_0 = \frac{L}{t_D E}\frac{P}{760}\frac{273.2}{T} \quad (5)$$

where P corresponds to the buffer gas pressure in Torr. The time required for ions to reach the detector is a composite of the drift time and the time required for ions to travel through other portions of the instrument. Thus, it is necessary to account for the flight times of ions when no gas is present as well as for

(24) Colby, S. M.; Reilly, J. P. *Anal. Chem.* **1996**, *68*, 1419.
(25) Mason, E. A.; McDaniel, E. W. *Transport Properties of Ions in Gases*; Wiley: New York, 1988.
(26) MATLAB Version 4, The Math Works Inc., Natick, MA, 1997.
(27) Revercomb, H. E.; Mason, E. A. *Anal. Chem.* **1975**, *47*, 970.
(28) Under low-field conditions, the diffusion constant is related to the measured mobility by the expression $D = Kk_bT/ze$, where K is the mobility, k_b is Boltzmann's constant, and ze is the charge.

differences in the ions' energies at the exit of the drift tube in the presence and absence of buffer gas. These corrections are small (~150−200 μs). Compact conformers have higher mobilities than more diffuse ones. The reproducibility of reduced mobilities is excellent. Any two measurements recorded on the same instrument on different days typically agree to within 1% (percent relative uncertainty). The reproducibility of data recorded consecutively is substantially better; positions of peak maximum usually agree to within 0.1%. The present experiments were carried out under low-field conditions where mobilities are independent of the applied drift field and drift velocities are small compared with the thermal velocity of the buffer gas. Under these conditions, ions are not expected to align in the drift tube.

RESULTS AND DISCUSSION

Nested High-Resolution Drift(Flight) Time Distribution for Tryptic Fragments. Figure 3 shows two-dimensional contour plots of drift times and m/z ratios for a mixture of peptides obtained from tryptic digestion of sheep albumin that were recorded using our low- and high-resolution ion mobility instruments. The main features in the spectra obtained from both instruments appear to be similar. The observed peaks are separated into two families of low-mobility $[M + H]^+$ and high-mobility $[M + 2H]^{2+}$ ions. Additionally, some ions arriving at shorter times than $[M + 2H]^{2+}$ ions of similar m/z are observed (especially apparent in Figure 3b).

Assignments of a few example peaks shown in Figure 3 were made by comparing measured m/z ratios (combined with the mobility-based assignment of charge state) with calculated masses for peptides that are expected to be formed from tryptic digestion. Detailed studies of tryptic fragments with the injected ion approach have been conducted.[29,30] For most small commercially available proteins (5−15 kDa) it is possible to assign 70−100% of the expected fragments with this approach; for larger proteins we typically observe 50% or more of the expected fragments. The low-resolution (injected-ion) configuration is well suited for studies of $[M + H]^+$ ions; the abundance of $[M + H]^+$ ions increases relative to the $[M + 2H]^{2+}$ ions as the energy used to inject ions into the drift tube is increased.[11] We have previously suggested that this behavior is due to an endothermic proton-transfer process (i.e., $[M + 2H]^{2+} + He \rightarrow [M + H]^+ + HeH^+$) that becomes energetically accessible because of a transient heating/cooling cycle that occurs during injection.[31] Collision-induced dissocation of the +2 ions would also influence the relative abundance of peaks. Two-dimensional integration of the injected ion data shows that $[M + H]^+$ ions comprise ~45% of the total observed ion signal (Figure 3). In the high-pressure, high-resolution drift tube, ions are thermalized during the electrospray process and drift at the buffer gas temperature into the ion mobility apparatus. This provides an extremely gentle means of sampling ions that is substantially more sensitive to higher charge states and fragile noncovalent structure.[32,33] The $[M + H]^+$ ions comprise only ~14% of the total ion signal in spectra collected using the high-pressure instrument.

The insets in Figure 3 show slices (ion mobility distributions) through the data at m/z values of 509, 538, and 704. Using the nested data acquisition approach and high-resolution instrument, most peaks for singly protonated peptide ions can be resolved at $t/\Delta t \approx 100-150$; higher resolving powers are observed for some peaks associated with multiply charged ions. This is a substantial improvement over $t/\Delta t$ values of 20−30, which are typical for the low-resolution configuration. The ion mobility slices that are shown are taken in regions where there are singly and doubly charged ions having nearly identical m/z ratios. The $m/z = 509$ slice includes contributions from the low-m/z portion of a peak corresponding to $[FGER + H]^+$ ($m/z = 508.554$) and the high-m/z side of the $[QTALVELLK + 2H]^{2+}$ ($m/z = 508.119$) ion peak. Peaks in the $m/z = 538$ slice are due to contributions from $[FWGK + H]^+$ ($m/z = 537.638$) and a small low-m/z tail associated with $[EGCFVLEGPK + 2H]^{2+}$ ($m/z = 540.128$). There are three resolved peaks in the $m/z = 704$ slice which correspond to the $[VLASSAR + H]^+$ ($m/z = 703.816$), $[LRCASIQKFGER + 2H]^{2+}$ ($m/z = 704.830$), and $[VGTKCCAKPESER + 2H]^{2+}$ ($m/z = 704.815$) ions. Although the m/z ratios for these ions are similar, each is easily resolved due to the large difference in mobility.

We note that the higher resolving power makes it possible to identify peptides and assign sequences to many peaks that could not be unambiguously assigned in the low-resolution data. For example the $[LRCASIQKFGER + 2H]^{2+}$ and $[VGTKCCAKPESER + 2H]^{2+}$ ions are easily resolved; these peptides cannot be distinguished in the low-resolution data (although a peak and shoulder are observed). Additionally, in the high-resolution data the $[TPVSEK + H]^+$ ($m/z = 660.745$) and $[QEPER + H]^+$ ($m/z = 658.689$) ions are resolved, whereas in the low-resolution data set, these ions are observed as a single broad peak. A number of larger, highly charged peptides that result from missed cleavages (primarily because of disulfide linkages) can also be identified in the high-resolution data. The improvement in resolving power makes it possible to separate multiple peptides within a charge-state family, a requirement for the analysis of peptide libraries.

Experimental and Predicted Mass Spectra for a (D)Phe-Xxx-Xxx-CONH$_2$ Library. Figure 4 shows a time-of-flight mass spectrum over a 150−600 m/z range recorded for the mixture of synthesized (D)Phe-Xxx-Xxx-CONH$_2$ library peptides. The most intense peaks, observed from $m/z = \sim 300$ to 550, are consistent with formation of a distribution of singly protonated (D)Phe-Xxx-Xxx-CONH$_2$ peptides. A broad low-intensity feature from $m/z = \sim 210$ to 320 is consistent with a distribution of $[$(D)Phe-Xxx-Xxx-CONH$_2 + 2H]^{2+}$ ions. Four distinct peaks are observed at low-m/z values (~163, 180, 187, and 197). There are several possible assignments for these peaks, including the following: groups of stable doubly charged peptides, singly charged impurities that result during synthesis (e.g., dipeptides formed by synthetic deletions, or combinations of residues and synthetic protecting groups), or dipeptides that arise from fragmentation of tripeptides.

It is instructive to compare the experimental mass spectrum with spectra that are calculated for peptides that are expected to be present in the mixture. Figure 5 shows a histogram plot of

(29) Valentine, S. J.; Counterman, A. E.; Hoaglund Hyzer, C. S.; Clemmer, D. E. *J. Phys. Chem. B* **1999**, *103*, 1203.

(30) Counterman, A. E.; Clemmer, D. E. *J. Am. Chem. Soc.* **1999**, *121*, 4031.

(31) The proton affinity of He is 42.5 kcal/mol, as given by: Lias, S. G.; Bartmess, J. E.; Liebman, J. F.; Holmes, J. L.; Levin, R. D.; Mallard, W. G. *J. Phys. Chem. Ref. Data* **1988**, *14* (Suppl. 1), 1.

(32) Hudgins, R. R.; Woenckhaus, J.; Jarrold, M. F. *Int. J. Mass Spectrom. Ion Processes* **1997**, *165*, 497.

(33) Li, J.; Taraszka, J. A.; Counterman, A. E.; Clemmer, D. E. *Int. J. Mass Spectrom. Ion Processes* **1999**, *185/186/187*, 37.

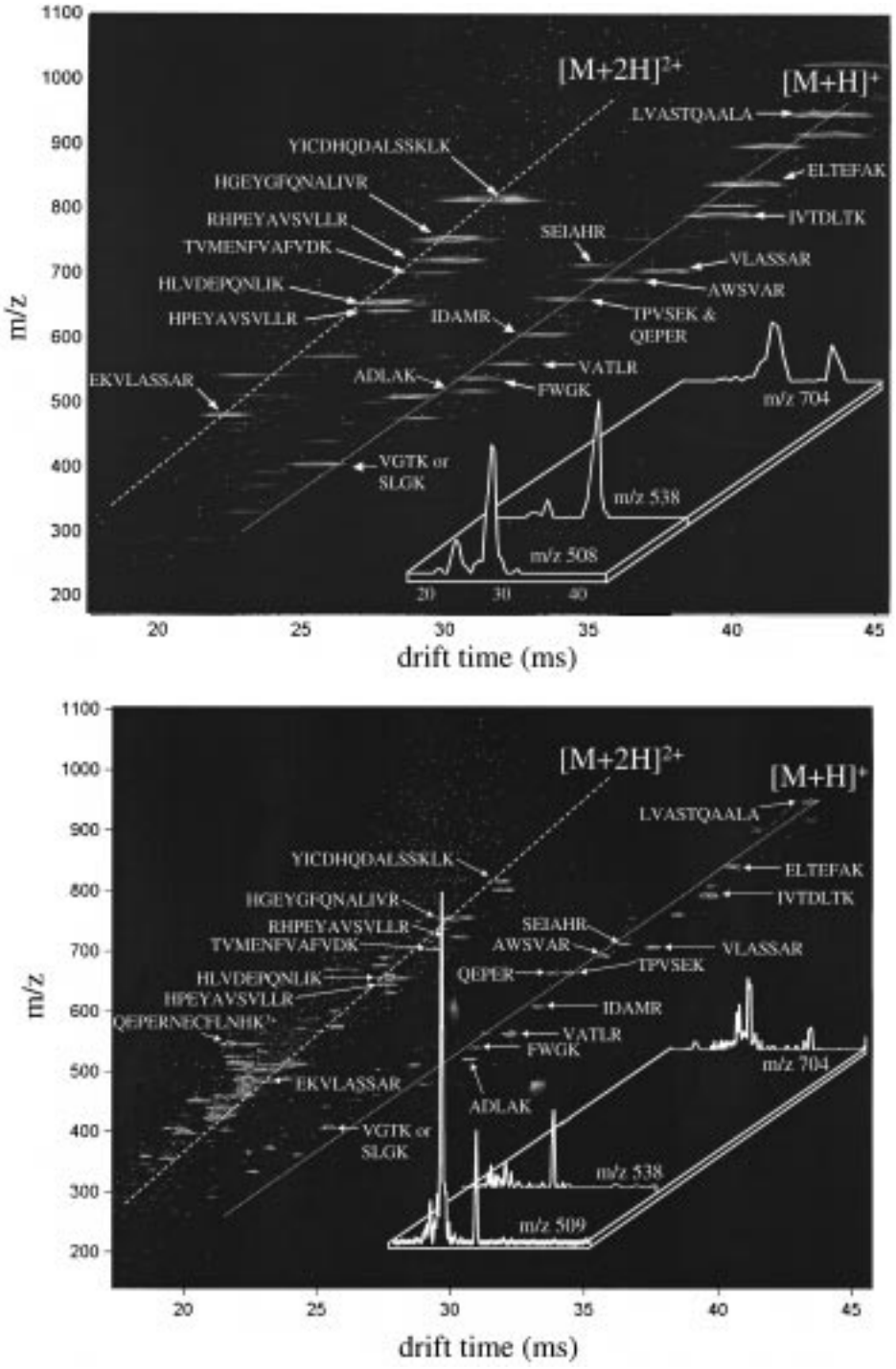

Figure 3. Contour plots of drift times and *m*/*z* ratios (determined from flight times) obtained upon electrospraying a mixture of peptides from a tryptic digest of sheep albumin. Part a (top) shows the distribution that is obtained when data are recorded using a low-resolution injected-ion drift tube (described in ref 11), where ion mobility separation was carried out using a buffer gas pressure of ~2.00 Torr and a drift field of 11.1 V cm^{-1} and subsequently scaled to the conditions used in part b. Part b (bottom) shows a plot of the same mixture of peptides when data are recorded using a high-resolution drift tube. These data were recorded using a buffer gas pressure of 162.2 Torr and a drift field of 137.4 V cm^{-1}. The insets show ion mobility slices take at m/z = 509, 538, and 704. See text for discussion.

expected ion intensities and m/z ratios (over an m/z range of 310−415). Peak intensities were obtained by binning peptides by their calculated $[M + H]^+$ ion m/z ratios into 0.1 increments.[34] Implicit in this calculation is that all peptides are present in equal abundance and have equal probability of forming singly protonated ions. Also shown is a calculated mass spectrum that has been convoluted over a mass resolving power ($m/\Delta m$) of 300, near the experimental resolving power. We calculate that 227 singly protonated peptides, distributed over 71 different 0.1 m/z bins

(34) Contributions from naturally occurring isotopes have been neglected in calculated mass spectra for these small ions.

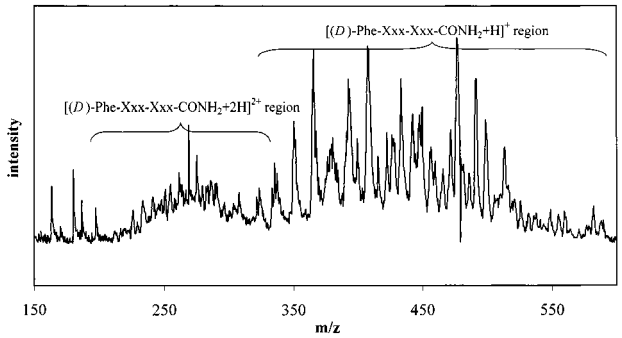

Figure 4. Time-of-flight mass spectrum obtained upon ESI of a mixture of Phe-Xxx-Xxx-$CONH_2$ library peptides. A mix and split strategy in which Xxx is randomized over 26 residues is expected to result in a mixture of 676 tripeptides. Regions that are expected to correspond to [(D)Phe-Xxx-Xxx-$CONH_2$ + H]$^+$ and [(D)Phe-Xxx-Xxx-$CONH_2$ + 2H]$^{2+}$ ions are labeled.

are present over the range shown in Figure 5. Peak intensities vary by as much as a factor of 8. The smallest peaks correspond to sequences where the second and third amino acids are identical [e.g., the (D)Phe-Pro-Pro-$CONH_2$ sequence having $m/z = 359.4$]. Intense peaks are found when many isomers are present, such as $m/z = 399.5$, where six sequence structural, or stereoisomer peptides (as indicated in the figure) are expected. Two additional sequences [(D)Phe-His-Pro-$CONH_2$ and (D)Phe-Pro-His-$CONH_2$] are expected at $m/z = 399.4$.

Figure 5 also shows a plot of the experimental mass spectrum over the same m/z range. The main experimental features are near the positions of large peaks in the calculated distributions. This suggests that many of the peptides expected from the mix and split synthesis must be present in the experimental data. However, these data do not provide quantitative information about the number and abundance of different components.

Nested Drift(Flight) Time Distributions for the (D)Phe-Xxx-Xxx-$CONH_2$ Library. Figure 6 shows a contour plot of nested ion mobility and m/z data for the electrosprayed (D)Phe-Xxx-Xxx-$CONH_2$ mixture. Peaks in the $m/z = \sim310-520$ and $\sim200-320$ regions can be grouped as low- and high-mobility families, respectively. Comparison of these families with the [M + H]$^+$ and [M + 2H]$^{2+}$ families in Figure 3b corroborates the assignment of these regions of the mass spectrum in Figure 4 as distributions of [(D)Phe-Xxx-Xxx-$CONH_2$ + H]$^+$ and [(D)Phe-Xxx-Xxx-$CONH_2$ + 2H]$^{2+}$ ions, respectively.

A distribution of very low intensity peaks with drift times of $\sim$19−24 ms ($m/z = \sim325-475$) also appears to correspond to doubly charged ions. These features were hidden under the large [(D)Phe-Xxx-Xxx-$CONH_2$ + H]$^+$ ion peaks in Figure 4. These ions have higher mobilities than those observed for the family of singly protonated ions and are consistent with formation of [((D)Phe-Xxx-Xxx-$CONH_2)_2$ + 2H]$^{2+}$ dimer ions. The observation that these peaks are observed in discrete positions suggests that these dimers are associated with interactions between specific pairs of monomers having favorable binding interactions. Several recent reports of the observation of specific favorable interactions between small peptides by ESI have been made;[35,36] the sensitivity of ESI to noncovalent associations in larger systems has been discussed extensively.[37] We cannot rule out the possibility that the peaks observed arise because of variations in the gas-phase stabilities of different pairs rather than specific solution-phase interactions.

A final note regarding the general assignment of features in Figure 6 involves the peaks observed at $m/z = 163$, 180, 187, and 197 that could be due to specific stable doubly charged peptides, synthetic impurities, or fragments. The nested data show that these ions arrive over a rather wide range of drift times ($\sim$14−19 ms). We rule out the possibility that these are doubly charged ions on the basis of their mobilities. These peaks could be due to a range of impurities associated with singly protonated deletion peptides, e.g., [Xxx-Xxx-$CONH_2$ + H]$^+$. It is also possible that these ions arise from fragmentation of tripeptides. In the latter case, it is likely that fragmentation is associated with [(D)Phe-Xxx-Xxx-$CONH_2$ + 2H]$^{2+}$ ions at the exit of the drift tube. Ion fragments formed after the drift tube (from collisions in the intermediate-pressure region before the mass spectrometer) would have drift times that are identical to their precursor parent ions, as is the case for the $m/z = 163-197$ peaks.

Figure 7 shows an expanded plot of the singly protonated family of ions, from $m/z = 375-505$. Drift times for different ions having identical (or very similar) m/z ratios vary by as much as $\sim$20%. Over this range 484 peptides, distributed over 260 m/z peaks (differing by more than 0.1 m/z), are expected. Depending on the threshold used in the contour plots (which has been varied from five to eight counts), we find evidence for $\sim$285−335 discernible features. This range should accurately reflect the number of different resolved species that are clearly above the noise level of the experiment. Many smaller peaks may not be included in this analysis. In most regions of the data, the number of discernible experimental peaks is slightly less than the number of peptides that are expected to be present in the library. An ion mobility slice at $m/z = 476.0$ reveals five peaks having roughly equal intensities. Six peptide sequences (as indicated in the figure) are expected. The similar relative intensity of each of the five resolved features suggests that only five of the six expected peptides are present in the mixture; however, we cannot rule out the possibility that two peptides (in lower abundance) have indistinguishable mobilities.

A second ion mobility slice at $m/z = 399.5$ is also shown in Figure 7. This slice is taken in a region that is substantially less intense than was expected on the basis of our calculated spectrum, where eight peptides (two at $m/z = 399.4$ and six at $m/z = 399.5$) were expected (Figure 5). Analysis of this ion mobility slice (as well as slices taken at other positions across the peak, m/z = 399.1 and 399.9) show that six different peaks are resolved. The peaks in this ion mobility slice are less intense than in most other regions of the spectrum. Numerous explanations could account for this behavior, including the following: suppression of [M + H]$^+$ peak intensity because of [M + 2H]$^+$ formation, which is likely for several of these sequences, which contain the relatively basic His and Pro residues,[38] and low synthetic yield of some peptide sequences. This behavior also occurs in several other regions of the spectrum indicating that the total number of different [M + H]$^+$ species that we have observed is below the

(35) Hudgins, R. R.; Jarrold, M. F. *J. Am. Chem. Soc.* **1999**, *121*, 3494.
(36) Lee, S.-W.; Beauchamp, J. L. *J. Am. Soc. Mass Spectrom.* **1999**, *10*, 347.
(37) For a recent review see: Smith, R. D.; Bruce, J. E.; Wu, Q.; Lei, Q. P. *Chem. Soc. Rev.* **1997**, *26*, 191.
(38) Hunter, E. P. L.; Lias, S. G. *J. Phys. Chem. Ref. Data* **1998**, *27*, 413.

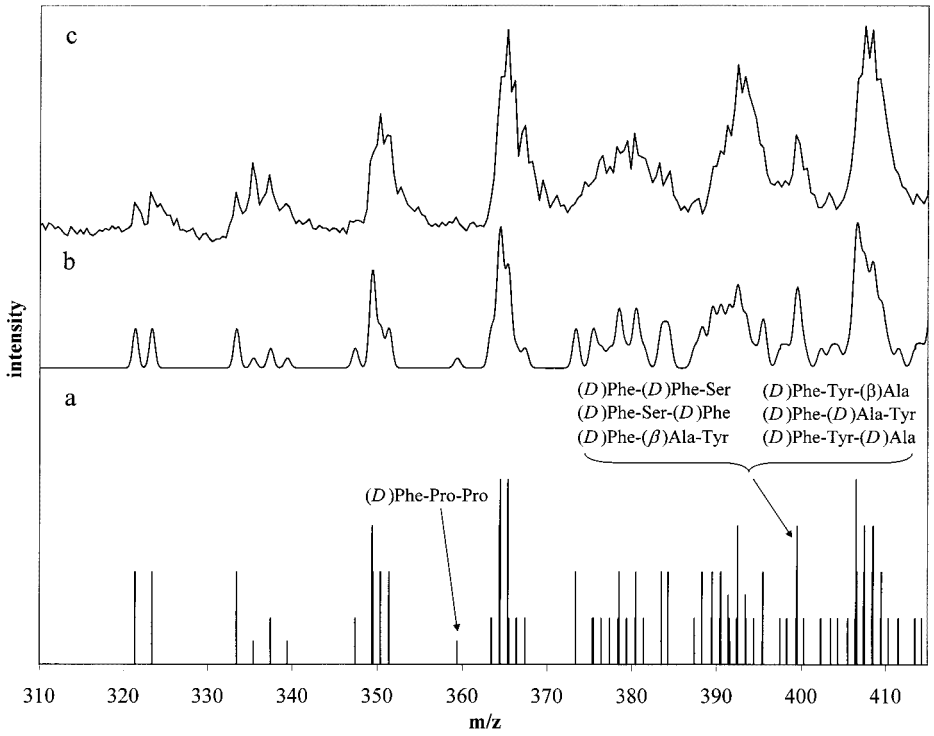

Figure 5. Part a shows a histogram of a calculated spectrum for peptides expected from the (D)Phe-Xxx-Xxx-$CONH_2$ library over a range of 310−415 amu. Peak heights are established by binning masses for expected peptides into 0.1 *m*/*z* increments. This assumes that concentrations and $[M + H]^+$ ionization efficiencies for all components are equal. Several sequences for specific peaks are indicated. Part b shows the calculated spectrum after it has been convoluted over a Gaussian peak shape corresponding to $m/\Delta m = 300$. Part c shows the experimental mass spectrum recorded over this range upon electrospraying a solution containing the mixture of library peptides.

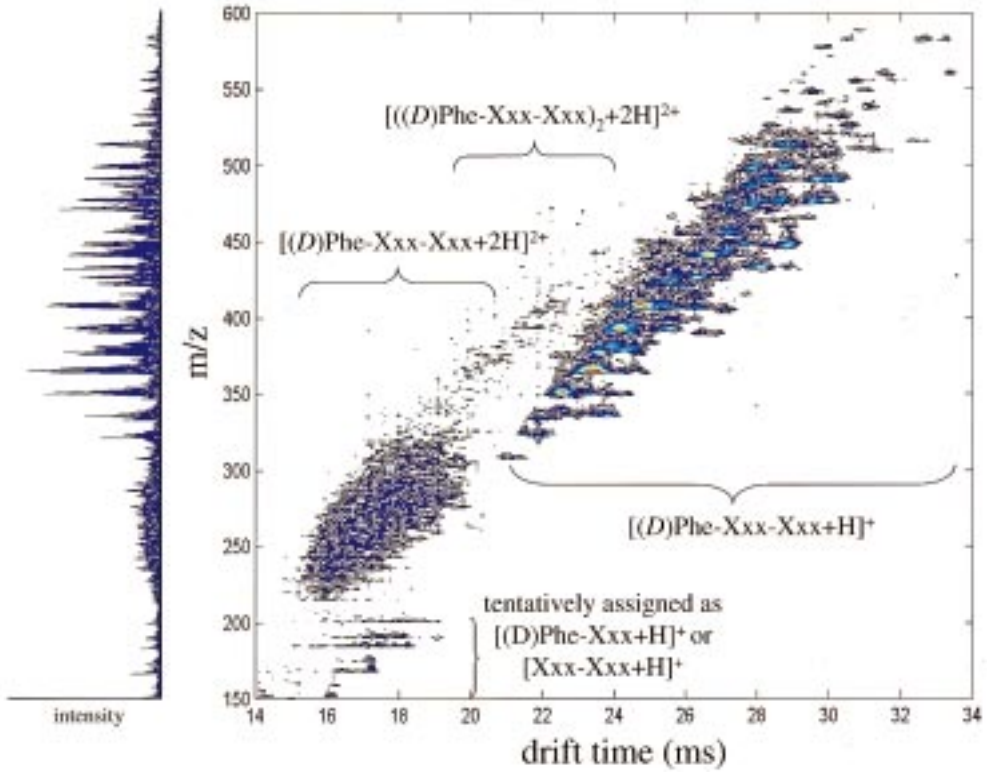

Figure 6. Contour plot of drift times and *m*/*z* ratios obtained for the mixture of (D)Phe-Xxx-Xxx-$CONH_2$ peptides. These data were recorded using an applied drift field of 137.4 V cm^{-1} and a He pressure of 164.5 ± 0.1 Torr. Regions that are expected to correspond to singly and doubly charged monomers, doubly charged dimers, and fragments are indicated. See text for discussion.

number that is expected on the basis of the mix and split protocol. From the number of different $[M + H]^+$ features observed over the entire spectrum, it appears that ~60−70% of the total number of expected peptides are present.

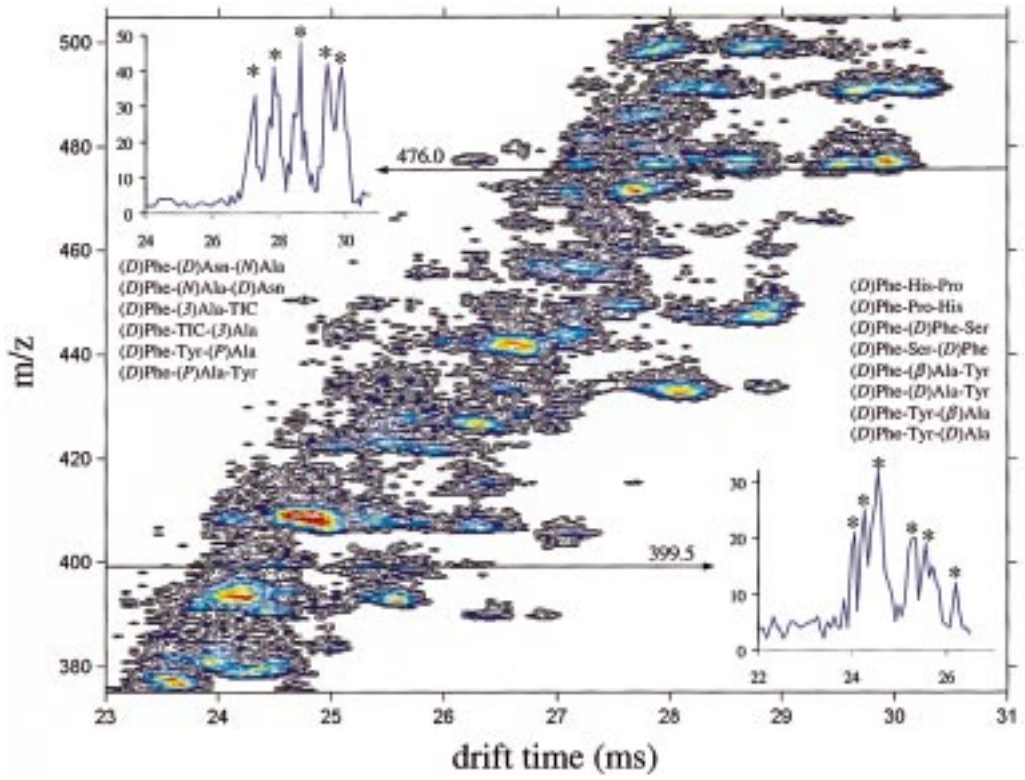

Figure 7. Contour plot of the nested data recorded for the (D)Phe-Xxx-Xxx-$CONH_2$ peptide library over an *m*/*z* range of 375−505. The insets show ion mobility slices (and peak intensities) taken at *m*/*z* = 399.5 and 476.0. Reproducible features are indicated with an asterisk. Sequences that are expected at these *m*/*z* ratios are indicated.

The data in Figure 7 also provide insight regarding the contributions of contaminants that arise from synthetic side reactions that occur during synthesis. Inspection of ion mobility slices at each *m*/*z* ratio shows that there are fewer resolved $[M + H]^+$ peaks than expected peptides in all but a few regions. Additionally, $[M + H]^+$ ion intensities in *m*/*z* regions where no peptides are expected are near the noise level of the experiment. This suggests that impurities due to side reactions are negligible in this system. By integrating appropriate regions of the two-dimensional spectrum, we estimate that less than 10% of the total ion signal is due to contaminants. In a final note, we have examined other types of libraries where side reactions appear to be problematic. These systems are still under investigation in our laboratory.[39]

SUMMARY AND CONCLUSIONS

A high-resolution drift tube has been combined with time-of-flight mass spectrometry for analysis of peptide mixtures, including a tryptic digest of sheep albumin and a library of three residue peptides having the general form (D)Phe-Xxx-Xxx-$CONH_2$ that was synthesized by a mix and split strategy and is expected to contain 676 different components. As noted previously, the mobility separation provides an effective means of reducing spectral congestion; peaks fall into families according to ion charge states.[10] Improvements in ion mobility resolving power have made it possible to distinguish between subtle mobility differences that occur within a charge-state family. Several groups have shown that high-resolution ion mobility methods are capable of resolving sequence isomers in small peptides. Hill and co-workers have separated several four-residue peptide sequence isomers.[40] Jarrold and co-workers have found that the position of a charged basic residue can stabilize or destabilize helix formation in alanine-based peptides, leading to large differences in mobilities.[35,41] We have recently shown that the intrinsic contributions to size of the isomeric Leu and Ile residues to peptide cross section can be discerned by ion mobility methods.[29] Using the present experimental configuration it appears to be possible to separate many sequence, structural, and stereo isomers. Approximately 60−70% of peptides that are expected to be present in the (D)Phe-Xxx-Xxx-$CONH_2$ library studied here can be observed as $[M + H]^+$ ions. Impurities due to side reactions are negligible, comprising <10% of the total $[M + H]^+$ signal.

The ability to resolve different $[M + H]^+$ isomers for a peptide library is an important first step in the application of gas-phase separations as a complementary strategy for MS analysis of complex mixtures. The present work underscores the need for a more detailed fundamental understanding of the relationship of observed $[M + H]^+$ peak intensities and actual solution composition. A number of recent studies indicate that peak intensities for small ions produced by ESI are relatively insensitive to matrix effects that occur during ionization,[4,42] suggesting that it may be possible to quantitatively define solution compositions from mass spectra. Matrix effects are clearly apparent during ESI of mixtures

(39) Srebalus, C. A.; Clemmer, D. E., unpublished results.

(40) Asbury, G. R.; Wu, C.; Siems, W. F.; Hill, H. H. Pittcon, 1998, New Orleans, LA, oral presentation of Abstr. 568.

(41) Hudgins, R. R.; Jarrold, M. F. *J. Am. Chem. Soc.* **1998**, *120*, 12974.

(42) Stephenson, J. L, Jr.; McLuckey, S. A. *J. Am. Soc. Mass Spectrom.* **1998**, *9*, 585.

containing large proteins (i.e., >40 kDa).[42] Because of the similarities in chemical properties, we expect sequence and stereo isomers to be relatively insensitive to matrix effects. However, as the diversity of different residues increases, it is unclear to what level it is appropriate to derive quantitative abundance information from $[M + H]^+$ peak intensities that are found using ESI.

Finally, by comparing experimental mobilities with calculated values for trial conformations that have been generated by molecular modeling methods, it should be possible to assign peaks in the ion mobility distribution to specific isomers. In this analysis, molecular modeling techniques would be used to generate distributions of structures for each ion expected from ESI of the mixture. For numerous atomic cluster systems,[43] small ion complexes,[16] and recently small peptide ions (including sequence isomers),[40,41,44] this approach has yielded convincing structural assignments. Assignments of specific mobility peaks for a group of isomers would be made by comparing calculated reduced mobilities to the experimental results.

(43) Wyttenbach, T.; Bushnell, J. E.; Bowers, M. T. *J. Am. Chem. Soc.* **1998**, *120*, 5098.

(44) See, for example: von Helden, G.; Hsu, M. T.; Kemper, P. R.; Bowers, M. T. *J. Chem. Phys.* **1991**, *95*, 3835. Jarrold, M. F. *J. Phys. Chem.* **1995**, *117*, 11.

ACKNOWLEDGMENT

We are indebted to Cherokee S. Hoaglund Hyzer, Anne E. Counterman (Indiana University), and Dr. Theodore Jones (Amgen) for many insightful comments regarding this work. We gratefully acknowledge Tom Zamborelli and Dr. John Mayers (Amgen) for technical support. Partial support of this work is from grants from the NSF (Career, CHE-9625199) and the NIH (1RO1GM55647-01).

Received for review April 9, 1999. Accepted June 28, 1999.

AC9903757